(2)

OFFICE OF NAVAL RESEARCH

GRANT NO. N00014-91-J-1447
R&T CODE 414044

Technical Report No. 21

DECOMPOSITION STUDIES OF TERTIARYBUTYLDIMETHYLANTIMONY

by

D.S. CAO, C.H. CHEN, C.W. HILL, S.H. LI, G.B. STRINGFELLOW,
D.C. GORDON, D.W. BROWN, and B.A. VAARTSTRA

Prepared for Publication

in the

Journal of Electronic Materials

University of Utah
Dept. of Materials Science & Engineering
Salt Lake City, UT 84112

May 22, 1992

Decomposition Studies of Tertiarybutyldimethylantimony

D. S. Cao, C. H. Chen, C. W. Hill, S. H. Li*, and G. B. Stringfellow
Dept. of Materials Science and Engineering
University of Utah
Salt Lake City, UT 84112

D. C. Gordon, D. W. Brown, and B. A. Vaartstra
Advanced Technology Materials, Inc.
7 Commerce Drive, Danbury, CT 06810

* Current Address: Solid-State Electronics Laboratory, Dept. of Electrical Engineering and Computer Science, University of Michigan, Ann Arbor, MI 48109

Abstract

The vapor pressure, decomposition temperature, decomposition products, and decomposition reaction order are reported for a novel organometallic vapor-phase epitaxy (OMVPE) Sb precursor, tertiarybutyldimethylantimony (TBDMSb, $C_4H_9(CH_3)_2Sb$). The TBDMSb vapor pressure is 7.3 torr at 23 °C. The 50% decomposition temperature is 300 °C for both He and D_2 ambients in a flow tube reactor with a residence time of approximately 3.2 seconds at 300 °C. The decomposition products are primarily C_4H_{10}, C_4H_8, and TMSb in both ambients. The overall decomposition reaction is first order. The decomposition mechanism is believed to be homolysis followed by recombination and disproportionation reactions for C_4H_9 and $(CH_3)_2Sb$ groups. Added trimethylgallium (TMGa) has no measurable effect on either the pyrolysis rate or the products. Apparently, TMGa and TBDMSb do not interact during pyrolysis nor do they form a room temperature adduct. No room temperature adduct between TMGa and TBDMSb was formed. It is believed that TBDMSb is a promising Sb precursor for low temperature OMVPE growth.

Key words: tertiarybutyldimethylantimony, TBDMSb, pyrolysis, decomposition, OMVPE, Sb source.

1. Introduction

Materials with bandgaps between 8 and 12 μm are desirable for far-infrared optoelectronic devices. An attractive system for such applications is InAsSbBi, which can be grown by organometallic vapor-phase epitaxy (OMVPE) [1]. For ternary InAsBi, it has been found that the Bi incorporation into the solid increases as the OMVPE growth temperature decreases [1]. 6% Bi in InAsBi has been achieved when the growth temperature was reduced to 275 °C [2]. At this temperature, the pyrolysis rate is very slow for the conventional Sb precursor trimethylantimony (TMSb) [3]. Thus, new Sb precursors are desired for low temperature growth of InAsSbBi and other Sb-containing III/V alloys.

Recently, several Sb precursors have been developed for this purpose. These include trivinylantimony (TVSb, $(C_2H_3)_3Sb$) [4], triisopropylantimony (TIPSb, $(C_3H_7)_3Sb$) [5], and triallylantimony (TASb, $(C_3H_5)_3Sb$) [5]. Since these precursors have relatively weaker alkyl-Sb bonds than methyl-Sb [6], they are expected to decompose at lower temperatures than for TMSb. Indeed, the values of 50% decomposition temperature (T_{50}) in He have been determined to be 460, 300, and 145 °C for TVSb, TIPSb, and TASb, respectively [4, 5]. These temperatures are all lower than the value of 510 °C observed for TMSb in He under the same conditions [3], consistent with the order of the Sb-C bond strengths [6].

Although the values of T_{50} for TVSb, TIPSb and TASb are lower than that of TMSb when the ambient is He, these precursors are not without problems. For TVSb, the value of T_{50} is unchanged when the He ambient is changed to H_2, the common ambient for OMVPE growth [4]. However, H_2 interacts with TMSb to accelerate the TMSb decomposition rate, lowering the value of T_{50} to 450 °C [3]. Thus, T_{50} for TVSb in H_2 is actually slightly higher than for TMSb, making the use of TVSb unattractive. On the other hand, TASb

decomposes at much lower temperatures. This suggests that TASb may be a useful Sb precursor for low temperature growth. Unfortunately, it apparently decomposes slowly during storage at room temperature [7], making it unappealing for practical use. The situation demonstrates the essential difficulty in developing a low temperature source: The precursor has to be stable at room temperature for long term storage, yet pyrolyze at approximately 250 °C in an OMVPE reactor to satisfy the requirements for the growth of alloys such as InAsSbBi, as discussed above. To date, only TIPSb has been successfully used to grow InSb at temperatures as low as 300 °C [8, 9].

In this work, the decomposition rate of another newly developed Sb source, tertiarybutyldimethylantimony (TBDMSb, $C_4H_9(CH_3)_2Sb$), is studied. TBDMSb is selected because it is expected to contain a weak C-Sb bond due to the stability of tertiarybutyl radicals, but still has reasonable vapor pressure due to the low overall molecular weight of the compound. The decomposition rate and the decomposition products as a function of temperature have been investigated in order to elucidate the pyrolysis mechanism. In addition, trimethylgallium (TMGa) has been added to the system to investigate possible interactions between the TBDMSb and group III precursors. This allows a preliminary appraisal of the possibility of using TBDMSb as an alternative Sb precursor for OMVPE growth.

2. Experimental

The experiments were conducted in an isothermal, flow-tube, SiO_2 reactor operated at atmospheric pressure (635 Torr in Salt Lake City), described in detail in Ref. [10]. The diameter and length of the reactor are 0.4 and 41.5 cm, respectively. The total gas flow rate was 40 sccm for the temperature dependence studies. This corresponds to a residence time in the

hot zone of 7.2 seconds at room temperature and 3.7 seconds at 300 °C. For the time dependence studies, the flow rate was varied between 20 and100 sccm. The effluent gas was sampled into a time-of-flight mass spectrometer via an adjustable leak. Both He and D_2 were used as carrier gases. D_2 was used to detect possible reactions of the precursor or the species produced during pyrolysis with the typical ambient used for OMVPE growth. The use of D_2 instead of H_2 allows one to label the products so that the reaction pathways can be identified more easily. In order to study the heterogeneous reactions on an SiO_2 surface, the reactor was packed with SiO_2 chips to increase the nominal surface area by a factor of 24. Since the heterogeneous reaction rate is proportional to the surface area, the effect of the increased surface area on the decomposition temperature will be significant if heterogeneous reactions are dominant.

To synthesize TBDMSb, an ether solution of TMSb was added to 2 equivalents of sodium in liquid ammonia, resulting in a dark red solution [11]. To this solution tertiarybutyl bromide was added. Evaporation of the ammonia and filtration to remove sodium bromide was followed by distillation, initially at atmospheric pressure to remove ether, and finally at reduced pressure to give TBDMSb as a colorless, air-reactive liquid. The compound was characterized by infrared spectroscopy, ^1H and ^{13}C nuclear magnetic resonance, and gas chromatography/mass spectroscopy.

The vapor pressure of TBDMSb was measured in a vacuum manifold equipped with a manometer (0-10 torr). The TBDMSb was degassed by multiple freeze-pump-thaw cycles. Then the TBDMSb vapor was allowed to equilibrate in the manifold. After equilibration, the TBDMSb ampule was closed off from the manifold, the manifold evacuated, and the equilibration repeated.

For the mass spectroscopic study, an ionization energy of 70 eV was used. Mass spectra for TBDMSb at room temperature were initially determined. Table 1 shows the relative abundances of the mass-spectral fragmentation peaks for TBDMSb in He at room temperature. The principal peak is at m/e=57, corresponding to $C_4H_9^+$. The peaks at m/e=121-195 belong to Sb^+, CH_3Sb^+, $(CH_3)_2Sb^+$, and $C_4H_9CH_3Sb^+$. Because Sb has two isotopes with masses of 121 and 123 with approximately equal concentrations [12], all these fragments show double peaks. The parent peak is also split, as observed at m/e= 208 and 210. Spectra for other reactants and products were acquired from the literature [13]. In calculating the concentration of a species, the ionization cross-sectional area for each molecule was assumed to be the sum of those of its constituent atoms [14].

3. Results and Discussion

The vapor pressure of TBDMSb was determined to be 8.1 torr at 26 °C, 7.3 torr at 23 °C, and 4.5 torr at 12 °C. The freezing point is approximately 8 °C and the boiling point is 56 °C at 50 torr. The vapor pressure vs. temperature relationship is shown in Fig.1. For comparison, Fig.1 also shows the temperature dependences of the vapor pressures of TMSb, TVSb, triethylantimony (TESb, $(C_2H_5)_3Sb$), TIPSb, and TASb [3, 4, 5, 15]. The TBDMSb vapor pressure is lower than that of TMSb, but is similar to that of TVSb and higher than those of other Sb precursors.

The percent decomposition of TBDMSb is plotted versus temperature in Fig.2. The data were obtained by monitoring the TBDMSb principal peak intensity at m/e=57. The percentage decomposition at each temperature is calculated according to equation (1):

$$\text{Decomposition (\%)} = (1-I_{57}/I^{\circ}_{57})\times 100 \qquad (1)$$

where I_{57} and I°_{57} are the intensities of peak 57 at the given temperature and at room temperature, respectively.

For the present experimental conditions, TBDMSb decomposition occurs in the 250-350 °C range, as seen in Fig.2. The decomposition rate of TBDMSb is unaffected when the ambient is changed from He to D_2. The decomposition temperature is lowered only slightly when the surface area is increased by a factor of 24, suggesting that the decomposition process is primarily homogeneous. For comparison, Fig.2 also shows the decomposition results for TMSb, TVSb, TIPSb and TASb in a He ambient. If a H_2 or D_2 ambient is used, the TMSb decomposition temperature is reduced by approximately 50 °C [3], while the decomposition rates for other precursors are unchanged. From Fig.2, it can be seen that the decomposition temperature for TBDMSb is similar to that for TIPSb.

Fig.3 shows the concentrations of the TBDMSb decomposition products, C_4H_{10}, C_4H_8, and TMSb, at several temperatures in He. It is seen that the C_4H_{10} and C_4H_8 concentrations are nearly equal. In addition to C_4H_{10}, C_4H_8, and TMSb, a weak peak at m/e=304, identified as $[(CH_3)_2Sb]_2$, is observed. The absolute concentration of $[(CH_3)_2Sb]_2$ cannot be determined since its fragmentation pattern is not available in the literature. It is only possible to show the peak intensity at m/e=304 as a function of temperature as seen in Fig. 4. It is seen that the $[(CH_3)_2Sb]_2$ disappears at high temperatures, probably due to pyrolysis.

An attempt was made to determine the concentration of C_8H_{18}. Because most of the mass-spectral fragmentation peaks for C_8H_{18} overlap those of C_4H_{10}, C_4H_8 and TBDMSb, the peak at m/e=99 was used (6% of the

principle peak at m/e=57 [13]). No peak at m/e=99 could be positively detected. Thus, the C_8H_{18} concentration is likely to be small.

The TBDMSb decomposition products are essentially unchanged at all temperatures when the ambient is D_2 rather than He. No deuterated products such as CH_3D were detected. The only difference between the products observed in the two ambients is that $[(CH_3)_2Sb]_2$ is produced in He but not in D_2. The reason for this difference is unclear.

The reaction order for TBDMSb decomposition in D_2 was determined from the time dependences of $\ln(I_{57}/I^\circ_{57})$ and $1/I_{57}-1/I^\circ_{57}$, as seen in Figs.5a and 5b. The relationship between $\ln(I_{57}/I^\circ_{57})$ and time is nearly linear, while that between $1/I_{57}-1/I^\circ_{57}$ and time is distinctly non-linear. Thus, the decomposition reaction is first order [16]. This suggests that Sb-C bond homolysis is the rate-determining step for TBDMSb decomposition.

The simplest model consistent with the experimental observations is expressed by the reactions:

$$C_4H_9(CH_3)_2Sb \rightarrow C_4H_9 + (CH_3)_2Sb \qquad (2)$$

$$2C_4H_9 \rightarrow C_4H_8 + C_4H_{10} \qquad (3)$$

$$(CH_3)_xSb + (CH_3)_ySb \rightarrow (CH_3)_{x+1}Sb + (CH_3)_{y-1}Sb \quad x,y=1,2. \qquad (4)$$

$$2(CH_3)_2Sb \rightarrow [(CH_3)_2Sb]_2 \ . \qquad (5)$$

Reaction (2) is simply homolysis of the tertiarybutyl C-Sb bond, which is expected to be the weakest bond in the molecule. The C_4H_9 radicals can then disproportionate to yield C_4H_8 and C_4H_{10} via reaction (3). The disproportionation reaction is a reasonable explanation of why the

concentrations of C_4H_8 and C_4H_{10} are nearly equal, as shown in Fig.3. Theoretically, it is possible that two C_4H_9 radicals could also recombine to form C_8H_{18}. However, since the concentration of C_8H_{18} is very small, we conclude that the recombination reaction is slow, so it is not listed.

Reaction (4) is the disproportionation reaction for Sb-bearing radicals. The ultimate products for these reactions are TMSb and Sb. The Sb produced would be deposited on the reactor walls so it would not be detected in the mass spectrometer. TMSb has indeed been observed, as shown in Fig.3. Reaction (5) is the recombination reaction for the dimethylantimony (DMSb, $(CH_3)_2Sb$) radicals. This reaction explains the observation of $[(CH_3)_2Sb]_2$. Tetramethyldistibine is known to decompose to produce Sb metal and TMSb [17]. This has been proposed to occur via the following reaction [18]

$$(CH_3)_2Sb + [(CH_3)_2Sb]_2 = Sb + 2\ TMSb\ . \qquad (6)$$

A similar reaction pathway has also been proposed for tetramethyldibismuthine [18]. The above reaction could explain why the observed concentration of tetramethyldistibine is small.

Based on the proposed mechanism, the TMSb concentration at complete decomposition should be equal to 2/3 of the input TBDMSb concentration. This is not the case, as seen in Fig.3. One source of error in the measured concentration is that the cross-sectional area (taken as the sum of the cross sectional areas for the individual atoms in the molecule) may be inaccurate. In addition, there may be pathways not discussed above for the disappearance of $Sb(CH_3)_n$.

In this model, no step is proposed to allow the DMSb produced in reaction (2) to lose its methyl ligands to yield free methyl radicals. This is because no CH_3D was observed experimentally for TBDMSb decomposition in

D_2. Based on previous results [3], CH_3 radicals would react with the D_2 to form CH_3D if they are present.

An attempt was made to estimate the relative reaction rates for DMSb homolysis as compared to the disproportionation reaction of two DMSb radicals. For the homolysis reaction,

$$(CH_3)_2Sb = CH_3 + (CH_3)Sb, \qquad (7)$$

it is assumed that the rate, R, is

$$R_7 = A \exp(-E_a/kT)\ C[(CH_3)_2Sb] \qquad (8)$$

where the prefactor A is taken to be 10^{16} sec^{-1}, the typical value for first bond fission in metal-alkyls [19], k is the Boltzman constant, T 's the temperature, and C(mole/l) is the concentration of $(CH_3)_2Sb$. The activation energy, E_a, is taken to be the average bond strength for the methyl-Sb bond in DMSb. In other words,

$$E_a = \frac{D_2 + D_3}{2} = \frac{(3 * (\frac{D_1 + D_2 + D_3}{3}) - D_1)}{2} \qquad (9)$$

where D_i is the energy required to break the i'th C-Sb bond in TMSb. The values for D_1 and $(D_1+D_2+D_3)/3$ are available in the literature [20]. The reaction rate for the disproportionation reaction,

$$2\ (CH_3)_2Sb = (CH_3)_3Sb + (CH_3)Sb \qquad (10)$$

is assumed to be collision-limited, i.e., the activation energy is assumed to be zero. This will give an upper limit for the reaction rate. The collision rate is estimated to be [21]

$$R_{10} = 10^9\ [C(\text{mole/l})]^2\ [\frac{T}{T_0}]^{1/2} \qquad (\frac{\text{mole}}{\text{sec-l}}) \qquad (11)$$

where C is taken to be the input TBDMSb concentration, T is the temperature and T_0 is room temperature. For these assumptions, the calculation yields a value of R_7/R_{10} on the order of 10^{-8} at 300 °C with even smaller values at lower temperatures. Although the estimation is done using several rough assumptions, the ratio R_7/R_{10} is small enough that it is reasonable to conclude that reaction (7) is negligible. This conclusion is somewhat unexpected, because for TMGa decomposition the opposite has been found to be true [22]. The main reason is that TMGa decomposes at higher temperatures than TBDMSb. The value of k_7 increases exponentially with increasing temperature so reaction (7) becomes more important than reaction (10) for TMGa decomposition.

For this model, reaction 2 is the rate-determining step for TBDMSb decomposition. Using the decomposition data from Fig.2 and the first-order kinetic rate law [16], rate constants for reaction (2) at various temperatures can be obtained, as displayed in the Arrhenius plot of Fig.6. A best fit gives:

$$\log k_2\ (s^{-1}) = 11.8 - 33.1\ (\text{kcal/mole})/2.303\ RT \qquad (12)$$

where R is the gas constant. The activation energy of 33.1 kcal/mole indicates the strength of the tertiarybutyl-Sb bond in TBDMSb. This value is comparable to that reported for the isopropyl-Sb bond in TIPSb [5]. This is consistent with the similar decomposition temperatures of TIPSb and TBDMSb, as seen in Fig.2. Theoretically, the tertiarybutyl-Sb bond should be weaker than the isopropyl-Sb bond due to the greater stability of tertiarybutyl radicals [23]. In comparing TIPSb and TBDMSb, however, an additional important factor is the steric crowding of the three isopropyl groups in TIPSb. This crowding

undoubtedly reduces the strength of the isopropyl-Sb bond. In TBDMSb, this crowding is much less severe due to the presence of the two small methyl groups. The net result is that the tertiarybutyl-Sb bond in TBDMSb is comparable in strength to the isopropyl-Sb bond in TIPSb.

To simulate OMVPE growth, TMGa was added to probe possible interactions between the group III and group V precursors in D_2. The value of T_{50} for TBDMSb in this case is 300 °C, the same as for TBDMSb decomposition without TMGa. The value of T_{50} for TMGa is 510 °C. This is the same value reported for TMGa decomposition alone in D_2 under the same conditions [22]. No adduct between TMGa and TBDMSb was detected at room temperature. In addition, the decomposition products for the TMGa+TBDMSb mixture in D_2 are the sum of those for TMGa and TBDMSb decomposition separately under similar conditions. It is concluded that TMGa and TBDMSb decompose independently when combined under these conditions.

4. Summary

The vapor pressure, decomposition temperature, decomposition products, and decomposition reaction order have been determined for TBDMSb. At 23 °C, the TBDMSb vapor pressure is 7.3 torr. TBDMSb decomposes homogeneously at 250-350 °C. The decomposition rate does not depend on the ambient gas. The major decomposition products include C_4H_{10}, C_4H_8, and TMSb in both He and D_2 ambients. An additional product, $[(CH_3)_2Sb]_2$, was observed in He. The overall decomposition reaction is first order. The decomposition mechanism is believed to be homolysis, producing C_4H_9 and $(CH_3)_2Sb$ radicals, followed by recombination and disproportionation reactions. When TMGa is added, TMGa and TBDMSb decompose independently with no interaction. They do not form a room

temperature adduct. These results indicate that TBDMSb is a promising Sb precursor for low temperature OMVPE growth.

5. Acknowledgments

This work was supported by Office of Naval Research and the Air Force Office of Scientific Research.

6. References

1. K. Y. Ma, Z. M. Fang, R. M. Cohen, and G. B. Stringfellow, J. Appl. Phys., 68 (1990) 4586

2. K. Y. Ma, Z. M. Fang, R. M. Cohen, G. B. Stringfellow, J. Appl. Phys., 70 (1991) 3940

3. C. A. Larsen, S. H. Li, and G. B. Stringfellow, Chemistry of Materials, 3 (1991) 39

4. C. A. Larsen, G. B. Stringfellow, and R. W. Gedridge, Jr., Chemistry of Materials, 3 (1991) 96

5. S. H. Li, C. A. Larsen, G. B. Stringfellow, and R. W. Gedridge, Jr., J. Electronic Materials, 20 (1991) 457

6. H. A. Skinner, Advances in Organometallic Chemistry, (F. G. A. Stone and R. West, Academic Press, N. Y., 1964) p.49

7. S.H. Li, and G. B. Stringfellow, unpublished data.

8. G. T. Stauf, D. K. Gaskill, N. Bottka, and R. W. Gedridge, Jr., Appl. Phys. Lett., 58 (1991) 1311

9. C. H. Chen, Z. M. Fang, G. B. Stringfellow, and R. W. Gedridge, Jr., paper presented at the Fifth Biennial Workshop on Organometallic Vapor Phase Epitaxy held at Panama City, Florida at April 14-17, 1991

10. N. I. Buchan, C. A. Larsen and G. B. Stringfellow, Appl. Phys. Lett., 51 (1987) 1024

11. H. A. Meinema, , H. F. Martens, and J. G. Noltes, J. Organometallic Chemistry, 51 (1973) 223

12. R. C. Weast, M. J. Astle, and W. H. Beyer, Eds., *CRC Handbook of Chemistry and Physics*, (CRC Press, Boca Ration, Florida, 1987)

13. F. W. McLafferty and D. B. Stauffer, *The Wiley/NBS Registry of Mass Spectral Data*, (Vol.1, John Wiley & Sons, N. Y., 1989)

14. J. W. Otvos and D. P. Stevenson, J. Am. Chem. Soc., 78 (1956) 546

15. G. B. Stringfellow, *OMVPE, Theory and Practice*, (Academic Press, Boston, 1989) p.31

16. O. Levenspiel, *Chemical Reaction Engineering*, 2nd. Edition, (John Wiley & Sons, Inc., N. Y., 1972) Chapter 2

17. A.B. Burg and L.R. Grant, J. Am. Chem. Soc. 81 (1959) 1

18. A.J. Ashe, E.G. Ludwig, and J. Oleksyszyn, Organometallics 2 (1983) 1859

19. G.P. Smith and R. Patrick, Int. J. Chem. Kinet. 15 (1983) 167

20. S.J.W. Price, in*Comprehensive Chemical Kenetics*, Sec.2, Vol.4, Edited by C.H. Bamford and C.F.H. Tipper (Elsevier, Amsterdam, 1972), Chap.4, pp197-257

21. G. B. Stringfellow, *OMVPE, Theory and Practice*, (Academic Press, Boston, 1989) p.146

22. C. A. Larsen, N. I. Buchan, S. H. Li, and G. B. Stringfellow, J. Crystal Growth, 102 (1990) 103

23. G. B. Stringfellow, *OMVPE, Theory and Practice*, (Academic Press, Boston, 1989) p.19

Table 1: Intensities of Mass Spectral Fragmentation Peaks for TBDMSb (0.6%) in He at 70 eV

M/e	Fragment	Rel. %
15	CH_3^+	2.3
27	$C_2H_3^+$	11.2
29	$C_2H_5^+$	55.0
39	$C_3H_3^+$	14.4
41	$C_3H_5^+$	36.8
57	$C_4H_9^+$	100.0
121	Sb^+	4.0
123	Sb^+	4.0
136	CH_3Sb^+	11.2
138	CH_3Sb^+	12.8
151	$(CH_3)_2Sb^+$	8.0
153	$(CH_3)_2Sb^+$	6.4
193	$C_4H_9CH_3Sb^+$	1.3
195	$C_4H_9CH_3Sb^+$	1.3
208	$C_4H_9(CH_3)_2Sb^+$	8.3
210	$C_4H_9(CH_3)_2Sb^+$	8.3

Captions:

Fig.1 Temperature dependence of vapor pressure for TMSb, TVSb, TBDMSb, TESb, TIPSb and TASb.

Fig.2 Temperature dependence of percent decomposition for TBDMSb. The results for TMSb, TVSb, TESb, TIPSb and TASb are also shown for comparison (open squares (□)). The TBDMSb decomposition results are shown as open circles (○) in a He ambient, filled circles (●) in a D_2 ambient, and crosses (+) in D_2 with a high surface area.

Fig.3 Temperature dependence of decomposition products for TBDMSb in He.

Fig.4 Peak intensity at m/e=304 (parent peak for $[(CH_3)_2Sb]_2$) as a function of temperature.

Fig.5 Time dependence of: (a) $\ln(I_{57}/I^{\circ}_{57})$ and (b) $1/I_{57}-1/I^{\circ}_{57}$ for TBDMSb decomposition in D_2.

Fig.6 Arrhenius plot of the TBDMSb pyrolysis rate constants in He and D_2.

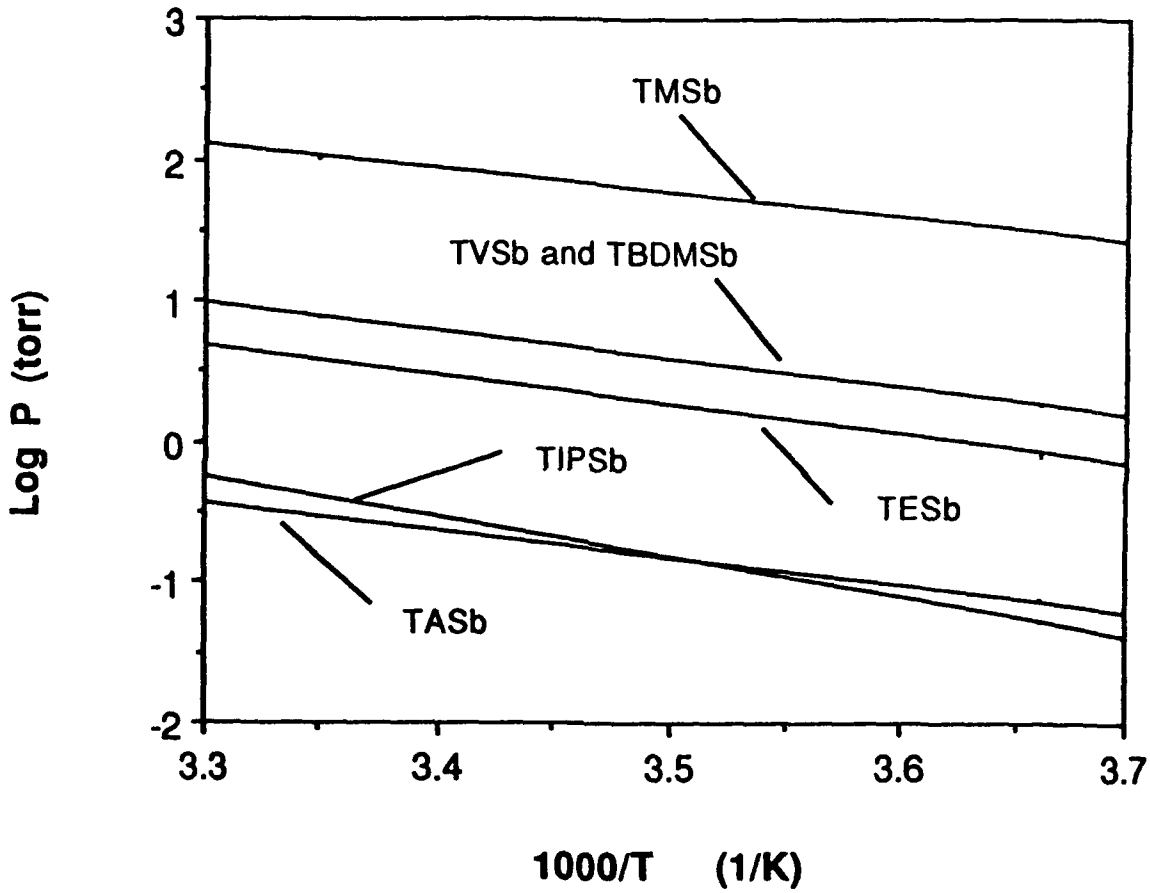
3
2
1
0
-1
-2
Log P (torr)
TMSb
TVSb and TBDMSb
TIPSb
TESb
TASb
3.3
3.4
3.5
3.6
3.7
1000/T (1/K)

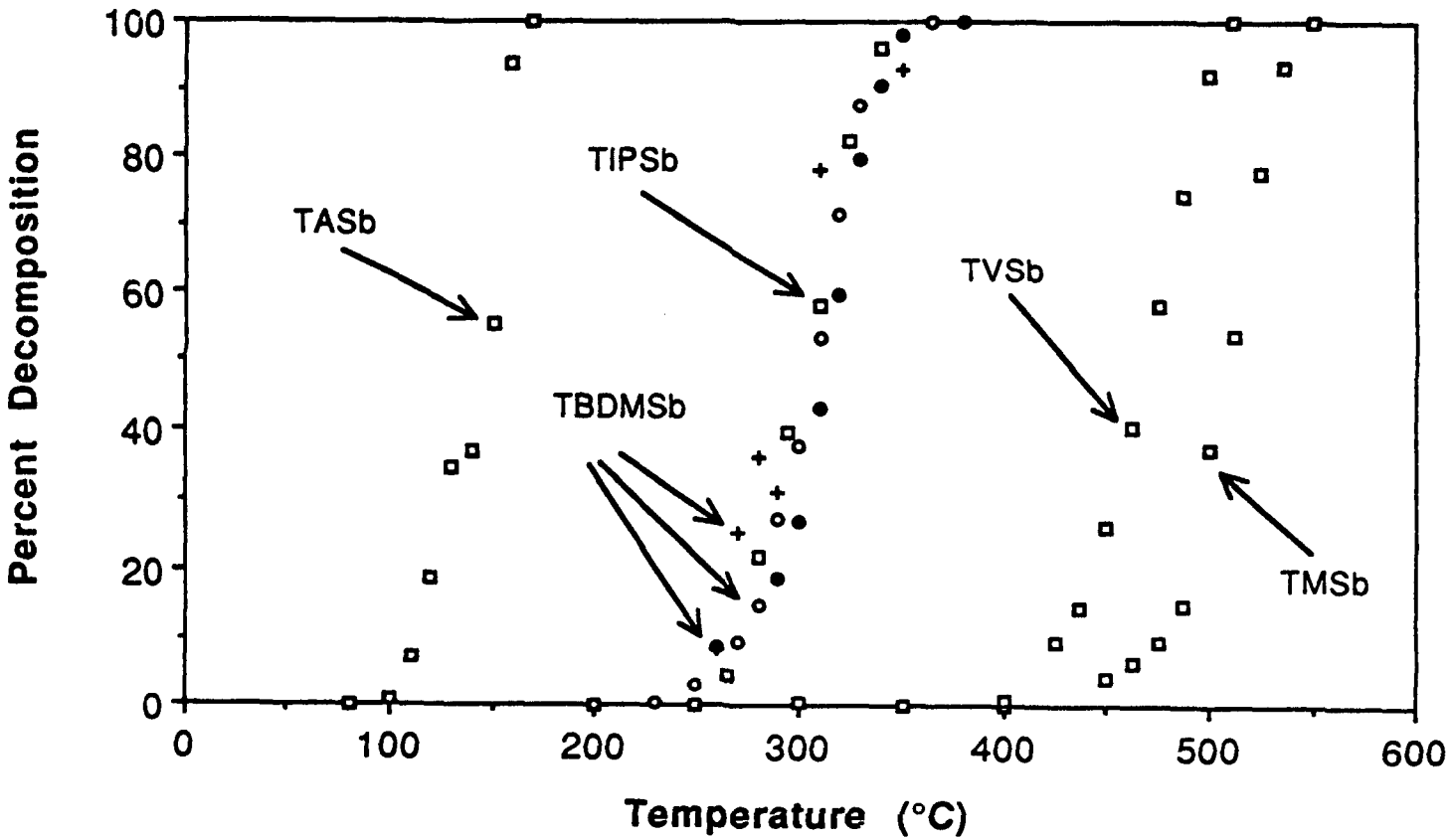
Percent Decomposition
100
80
60
40
20
0
0
100
200
300
400
500
600
Temperature (°C)
TASb
TIPSb
TBDMSb
TVSb
TMSb

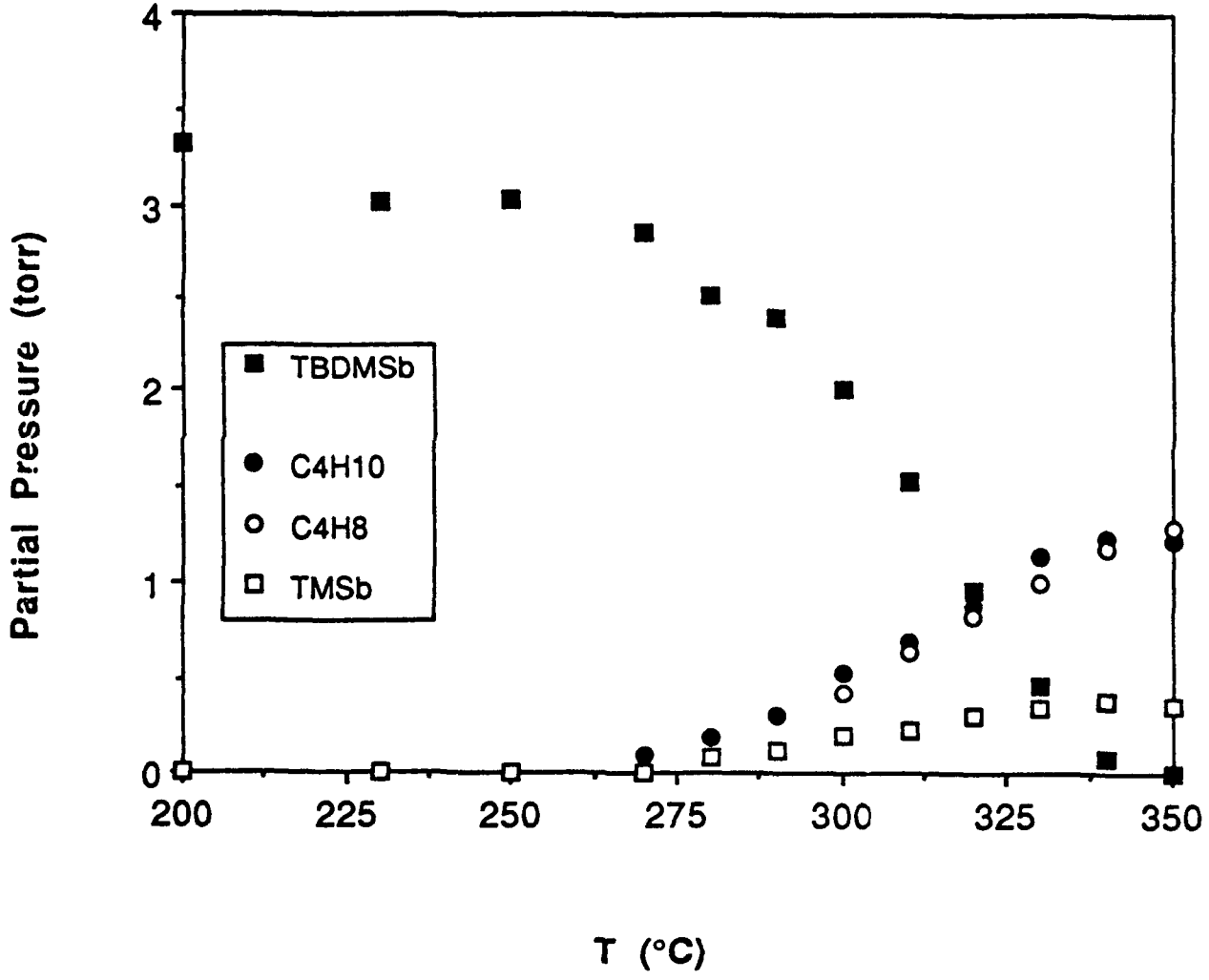
Partial Pressure (torr)
4
3
2
1
0
200
225
250
275
300
325
350
T (°C)
TBDMSb
C4H10
C4H8
TMSb

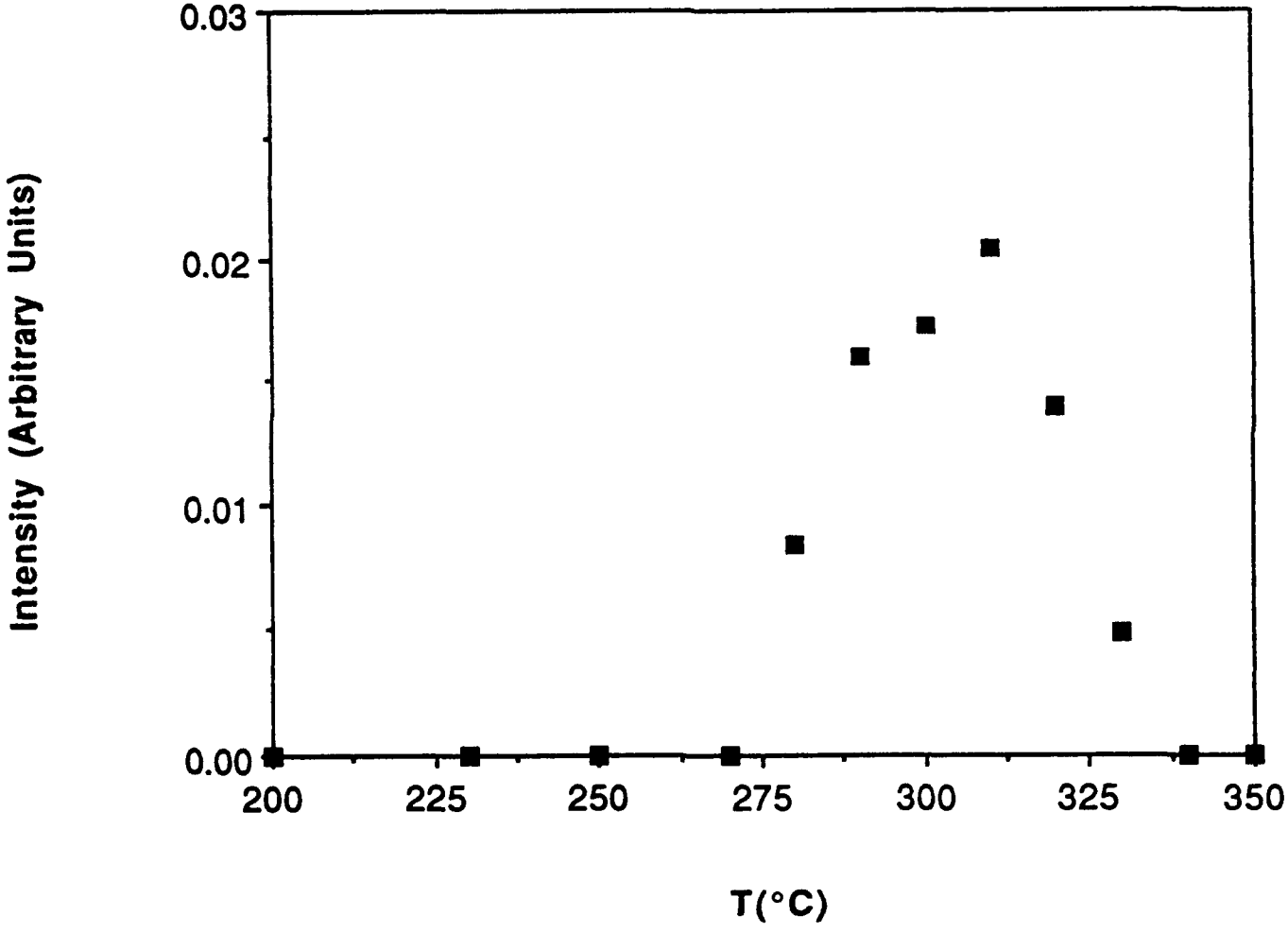
0.03
0.02
0.01
0.00
Intensity (Arbitrary Units)
200
225
250
275
300
325
350
T(°C)

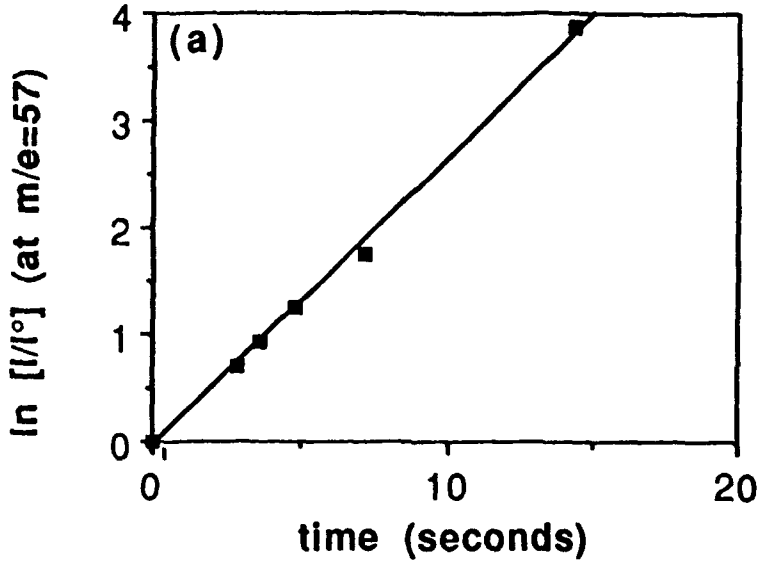
(a)
ln [I/I°] (at m/e=57)
4
3
2
1
0
0
10
20
time (seconds)

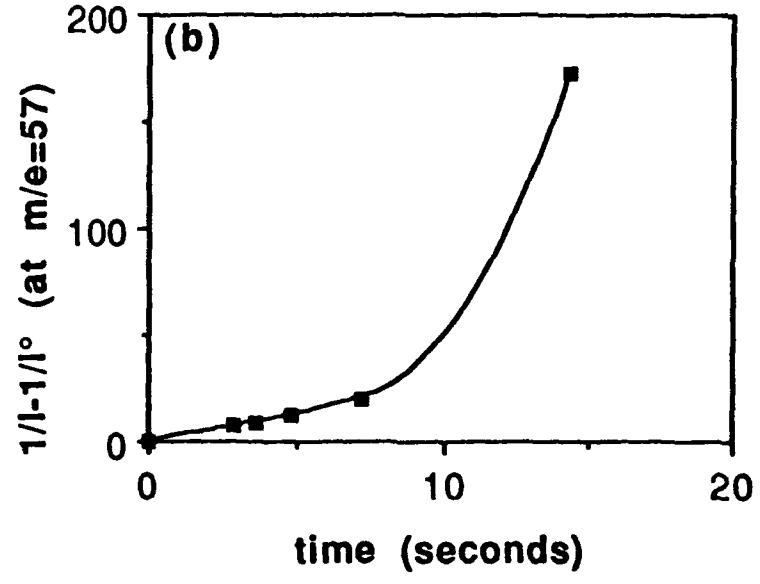
(b)
1/I-1/I° (at m/e=57)
200
100
0
0
10
20
time (seconds)

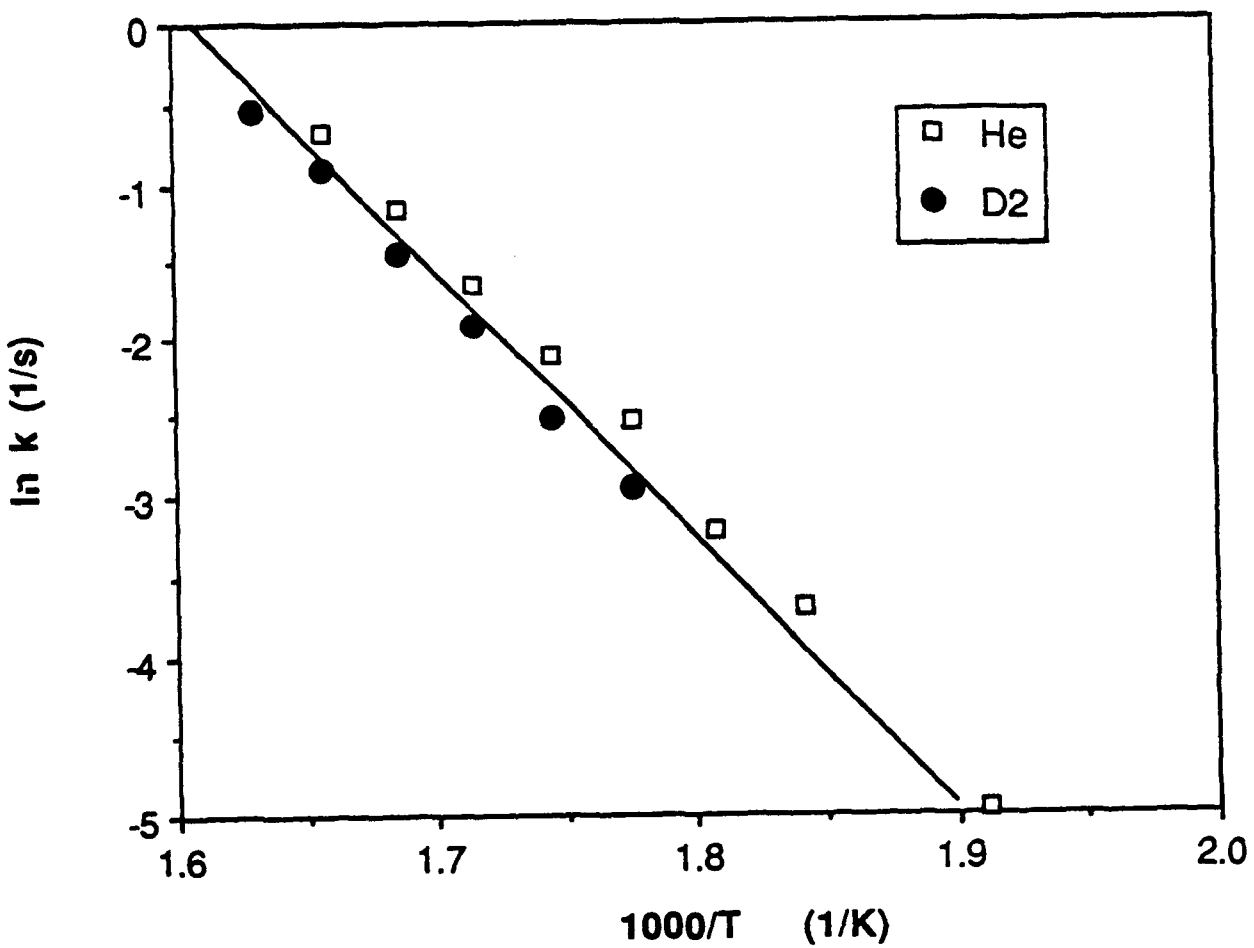
0
-1
-2
-3
-4
-5
ln k (1/s)
1.6
1.7
1.8
1.9
2.0
1000/T (1/K)
He
D2